Chemical Engineering Journal 154 (2009) 25–33

Contents lists available at ScienceDirect

Chemical Engineering Journal

journal homepage: www.elsevier.com/locate/cej

Kinetics of free fatty acids esterification: Batch and loop reactor modeling

R. Tesser, L. Casale, D. Verde, M. Di Serio, E. Santacesaria *

Dipartimento di Chimica, Università degli Studi di Napoli Federico II, Via Cinthia, Complesso Universitario di Monte di Sant'Angelo, 80126 Napoli, Italy

ARTICLE INFO

Article history:
Received 2 December 2008
Received in revised form 19 February 2009
Accepted 8 March 2009

Keywords:
Biodiesel production
FFAs esterification
Ion-exchange resins

ABSTRACT

Biodiesel is a fuel derived from a renewable vegetable origin and is object of growing interest in recent years both as a pure fuel and as blending component to reduce exhaust pollutants of traditional diesel fuel. The conventional biodiesel production technology involves the use of alkaline catalysts and is therefore not compatible with large amounts of free fatty acids (FFAs) and moisture in the feedstock due to the formation of soaps that strongly affect the feasibility of glycerol separation by liquid–liquid splitting. A preliminary stage of acidity reduction is therefore necessary, for this process, if the starting material is characterized by a free acidity higher than 0.5% by weight often contained in cheaper feedstock which lowers the production costs. This can be pursued, for example, by means of an esterification reaction of the FFAs with methanol, catalyzed by ionic-exchange sulphonic acid resins. In the present work, the above-mentioned reaction has been studied in different reactor configurations on a model mixture composed by artificially acidified soybean oil with oleic acid using an acid exchange resin as catalyst. This work has been developed in two parts: (i) a kinetic study in batch conditions with the purpose of developing a suitable kinetic expression and determining the related parameters and (ii) a study of the FFAs esterification in a packed bed tubular reactor operated inside a circulation loop. The kinetic model that is developed on the basis of several batch runs is able to simulate also the behavior of dynamic tubular loop reactor, providing that the external mass transfer resistance is properly accounted for. The mass transfer coefficient is satisfactorily modeled using correlations available on literature.

1. Introduction

The worldwide interest toward biofuels has recently significantly grown as a direct result of the renewed need of facing the global warming effect by reducing the greenhouse gases emissions that are related to the wide use of fossil fuels. In this respect, biodiesel represents a valuable alternative to petroleum-derived fuels due to both its renewable nature and its substantially reduced net carbon dioxide emission. This biofuel is conventionally produced through batch or continuous transesterification of refined vegetable oils with methanol by using homogeneous alkaline catalysts such as sodium or potassium hydroxides or methoxides [1,2]. Glycerol is the co-product of this reaction in a ratio of 10% by weight of the oil (1:1 molar ratio with triglyceride). The mentioned technology, however, is only compatible with highly refined oils which free fatty acids (FFAs) content does not exceed the threshold value of about 0.5% by weight. As a matter of fact, FFAs in the presence of an alkaline catalyst, give place to soaps forming stable emulsions between biodiesel and glycerol characterized by a long settling time for the complete separation of the two liquid phases. The main limitation for a wider biodiesel market share is therefore represented by the relatively high raw material cost: the steps of production, transportation, storage and refining of vegetal oils affect for more than 85% of the total biodiesel cost [3] making biodiesel by the conventional production technology significantly more expensive than diesel oil from petroleum.

A possible solution to this drawback could consist in the development of new technologies enabling to employ waste raw materials such as fried oils or oleins from various sources that cannot be treated in the conventional process for their high content in free fatty acids. This perspective is very interesting and discloses the way toward the development of innovative biodiesel production processes such as those based on supercritical methanol [4], or the two-stage process (esterification and transesterification reaction) [5,6]. In the two-stage process, the oil acidity is reduced below the acceptable limit by an esterification pre-treatment with methanol (acid catalyzed) producing methylesters (biodiesel) and water while, in the subsequent step, the traditional transesterification (base catalyzed) can be performed producing biodiesel and glycerol. The esterification reaction of acid oils or animal fats can then be used both as biodiesel direct production (in the case of substrates at very high content of FFAs) and as pre-treatment step in the framework of a conventional transesterification process (for feedstock with moderate free acidity). The generic esterification

* Corresponding author. Tel.: +39 081 674027; fax: +39 081 674026.
E-mail address: elio.santacesaria@unina.it (E. Santacesaria).

1385-8947/$ – see front matter © 2009 Elsevier B.V. All rights reserved.
doi:10.1016/j.cej.2009.03.010

Nomenclature

a	acidity (wt% in oleic acid)
a_S	specific interface area ($cm^2\ cm^{-3}$)
b	adsorption equilibrium constant ($cm^3\ mol^{-1}$)
C	concentration ($mol\ cm^{-3}$)
C_{titr}	concentration of titrant ($mol\ cm^{-3}$)
C_{cat}	concentration of catalyst ($g_{cat}\ cm^{-3}$)
d_p	particles average diameter (cm)
E_A	activation energy ($kcal\ mol^{-1}$)
k	kinetic constant of uncatalyzed reaction ($cm^6\ mol^{-2}\ min^{-1}$)
k_{cat}, k_{-cat}	kinetic constants of the forward and the reverse reaction (PH model, $cm^6\ mol^{-1}\ g_{cat}{}^{-1}\ min^{-1}$) (ER model, $cm^3\ g_{cat}{}^{-1}\ min^{-1}$)
k_S	mass transfer coefficient ($cm\ min^{-1}$)
M	molecular weight ($g\ mol^{-1}$)
m	mass of component initially charged (g)
m_{sample}	weight of sample (g)
N	number of experimental data
n	number of moles (mol)
Q_R	circulation flow rate ($cm^3\ min^{-1}$)
R	universal gas constant ($kcal\ mol^{-1}\ K^{-1}$)
r_{cat}	rate of catalyzed reaction ($mol\ min^{-1}\ g_{cat}{}^{-1}$)
r_{uc}	rate of uncatalyzed reaction ($mol\ min^{-1}\ cm^{-3}$)
Re_p	particle Reynolds number
RMS	root mean square error
Sc	Schmidt number
Sh	Sherwood number
T	temperature (K)
t	time (min)
U^B	linear velocity in the bed ($cm\ min^{-1}$)
V	volume (cm^3)
V_{titr}	volume of titrating solution (cm^3)
W_{cat}	weight of catalyst (g)
ε	bed void fraction
ν	stoichiometric coefficient
ρ_{mix}	density of the mixture ($g\ cm^{-3}$)
η_{mix}	viscosity of the mixture ($g\ cm^{-1}\ min^{-1}$)

Subscripts

A	oleic acid
E	methyl ester
i	index for ith component
j	index for jth cell
L	liquid
M	methanol
out	exit of tank or of packed bed reactor
W	water

Superscripts

B	packed bed reactor
C	cell
$calc$	calculated value
exp	experimental data
R	tubular reactor without catalyst
ref	reference temperature, 373.16 K
S	surface of catalyst
T	tank reactor
TOT	total volume

reaction of a carboxylic acid with methanol, producing methylester and water, is schematically shown below:

$$\underset{(A)}{RCOOH} + \underset{(M)}{CH_3OH} \rightleftarrows \underset{(E)}{RCOOCH_3} + \underset{(W)}{H_2O}$$

The esterification processes for FFAs abatement are generally based on homogenous acid catalyzed reaction [5,6] or by ionic-exchange acid resins as heterogeneous catalysts. As example, Pasias et al. [7] have investigated the FFAs esterification reaction catalyzed by Purolite resin and have interpreted their kinetic data by using a pseudo-homogeneous equilibrium model, frequently used in literature for similar systems due to its simple form.

Marchetti et al. [8] have studied this reaction by using, on the contrary, basic resins as catalysts like Dowex monosphere 550 A and Dowex upcore Mono A-625 obtaining interesting results, but without a modeling approach. Tesser et al. [9] reported the esterification reaction kinetics of oleic acid with methanol in the presence of triglycerides, catalyzed by acid resin Resindion Relite CFS in a batch reactor. Furthermore, Santacesaria et al. [10,11] have shown that the esterification reaction, performed in a continuous packed bed tubular reactor (PBR), was strongly affected by external mass transfer limitations while good results can be achieved by adopting alternative reactor configurations represented by the well stirred slurry reactor (WSSR) and the spray tower loop reactor (STLR). In fact for this operation, tubular packed bed reactors requires long residence times due to the relatively low reaction rates. In these conditions low volumetric flow rates are required resulting in very low Reynolds numbers at which the external fluid-to-solid mass transfer resistance can become significant in comparison with the intrinsic kinetics. This is the main reason for the discrepancy frequently observed between the experimental behavior of a tubular reactor and its simulation based upon the kinetics developed from batch runs.

However, it is possible to consider an alternative configuration in which a tubular packed bed reactor can usefully be operated inside a circulation loop around a reservoir tank, to provide high flow rates. In this case the per-pass conversion could be relatively low but the external mass transfer resistance will be minimized or eliminated due to the high interstitial fluid velocity.

As a prosecution of a previous experimental activity on a different exchange resin as catalyst [9–11], in the first part of the present work a deepened kinetic analysis of the esterification reaction of oleic acid with methanol in the presence of triglycerides (soybean oil), catalyzed by Amberlyst 15, will be reported. Amberlyst 15 is a cationic resin with acid character frequently used for promoting the esterification reaction of simpler substrates such as acetic acid with different alcohols and in different reactor configurations [12–15].

In the present work, results from the batch experiments are interpreted by both a pseudo-homogeneous and Eley-Rideal model. The comparison and the discrimination between the two models has been performed on the basis of statistical analysis.

In the second part of the work, experimental runs are performed in a tubular packed bed reactor operated inside a circulation loop. The experimental data have been modeled by using the kinetic expression and parameters, evaluated in batch conditions in the first part of the work and introducing a mass transfer coefficient calculated by using a literature dimensionless correlation.

In conclusion, we have demonstrated that in the packed bed loop reactor, by operating at a sufficiently high recirculation flow rates, the kinetic regime could be approached as it occurs in the well stirred batch reactor but without the inconvenience of breaking the catalyst particles.

Table 1
Typical properties of Amberlyst 15 resin.

Matrix	Macroreticular copolymer styrene-DVB
Physical form	Opaque beads
Ionic form as shipped	Hydrogen
Concentration of active sites	>1.7 equiv./L >4.7 equiv./kg
Moisture holding capacity	52–57% (H^+ form)
Shipping specific weight	770 g/L (48 lbs/ft^3)
Particles size	
Uniformity coefficient	<1.70
Harmonic mean size	<0.600–0.850 mm
Fine contents	<0.355 mm: 1.0% max
Coarse beads	>1.180 mm: 5.0% max
BET analysis	
Surface area	53 m^2/g
Average pore diameter	300 Å
Total pore volume	0.40 ml/g

2. Experimental

2.1. Reactants and methods

The used reactants and the related purities are the following: methanol (Carlo Erba, purity 99.9%, w/w), oleic acid (Carlo Erba, purity 99.9%, w/w), and a commercially available acidity-free soybean oil (acidity <0.3%, w/w).

The sulphonic acid resin, used as catalyst, has been purchased by Acros Organics and its characteristics are reported in Table 1. Before the experimental runs, resin has been dried at 100 °C for 24 h in a ventilated oven and fresh catalyst was used in each batch run.

The withdrawn samples were analyzed by a standard acid-base titration procedure for the evaluation of the free residual acidity. The analysis repeatability has been improved by removing methanol in excess and water formed, in a oven heated at 150 °C under stirring for 15 min, prior to submitting the samples to titration.

A weighed amount of the sample was then dissolved in ethanol, some droplets of phenolphthalein as indicator were added, and the titration is then performed by means of an alkaline 0.1 M KOH solution. The volume of alkaline solution consumed is recorded, and the acidity of the sample can be calculated by means of the following relation:

$$a\ (\text{wt\%}) = \frac{V_{titr} \cdot C_{titr} \cdot M_A}{m_{sample}} \times 100 \quad (1)$$

The acidity evaluated by Eq. (1) is referred to the oil phase (triglyceride + oleic acid + ester) with an error less than 1–2% on the free acidity expressed as weight percent of oleic acid.

2.2. Batch reactor

The scheme of the experimental apparatus used for batch runs is reported in Fig. 1. The device is composed by a stainless steel tank reactor (volume 0.6 l) equipped with a magnetically driven stirrer and with pressure and liquid phase temperature indicators. The reactor temperature is maintained at the prefixed value, within ±1 °C, by means of an electrical heating device connected to a PID controller. The reactor body is connected to a stainless steel pressurized chamber with a volume of 150 ml by means of which methanol can be added to the reaction system. The system is initially charged with the desired amount of acid oil and catalyst and, when the temperature reached the desired value, methanol is added using a nitrogen overpressure. This instant represents the initial time for the reaction. During the run, small samples of liquid phase were withdrawn by using a line equipped with a stopping valve. In this way the evolution with time of the mixture acidity can be monitored for different reaction times.

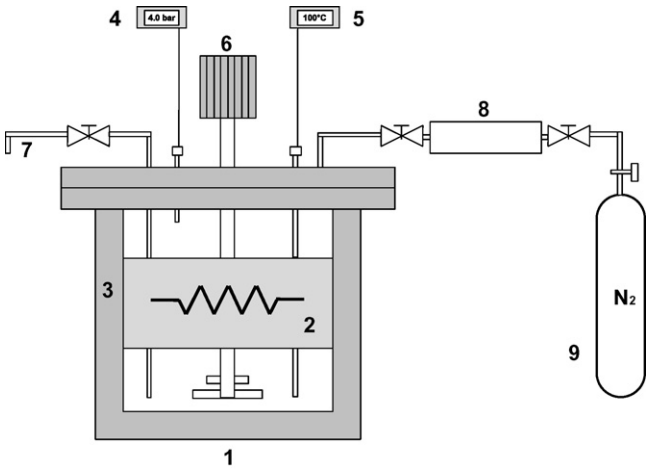

Fig. 1. Batch reactor experimental apparatus. (1) Reactor; (2) heating device; (3) rock wool thermal insulation; (4) pressure transducer and indicator; (5) liquid phase thermocouple; (6) magnetically driven stirring device; (7) sampling line; (8) stainless steel pressure chamber for methanol addition; and (9) nitrogen cylinder.

2.3. Packed bed loop reactor

The scheme of the experimental apparatus corresponding to a packed bed loop reactor is reported in Fig. 2. The system is composed by a stainless steel tank (AISI 316) with a total volume of 1 l, heated by a thermoresistance controlled by an electronic PID device. The stirring of the liquid in the tank is ensured by a magnetically driven stirrer and the bottom of this tank is connected, through a recirculation piston pump, to the packed bed reactor. The reactor has an external diameter of 0.5 in. and a length of about 330 mm. The packing of the reactor is formed by mixing together the cat-

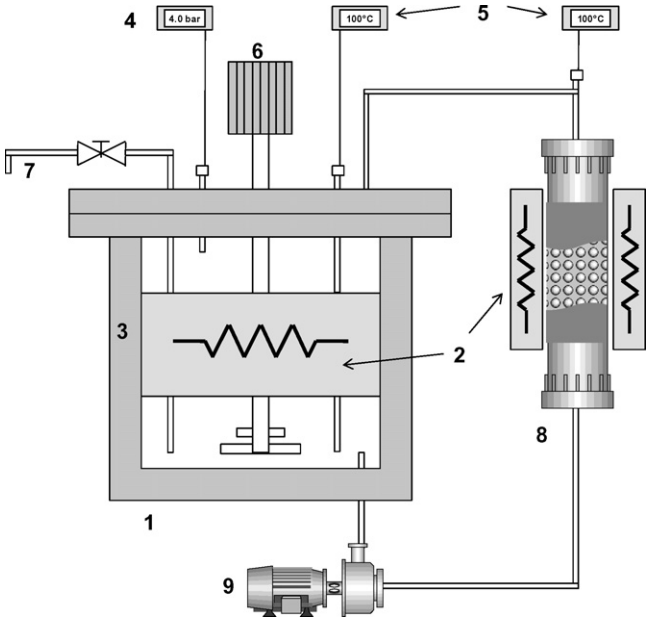

Fig. 2. Loop reactor experimental apparatus. (1) Reservoir tank; (2) heating devices; (3) rock wool thermal insulation; (4) pressure transducer and indicator; (5) thermocouples for tank liquid phase and outlet of tubular reactor; (6) magnetically driven stirring device; (7) sampling line; (8) tubular packed bed reactor; and (9) circulation pump.

Table 2
Operative conditions of experimental runs in batch reactor.

Run	Temperature (°C)	Initial pressure (bar)	Amount of catalyst (g)	Amount of soybean oil (g)	Amount of oleic acid (g)	Initial acidity (%)	Amount of methanol (g)
1	100	4.3	Uncatalyzed	101.8	98.2	49.1	89.1
2	120	5.1	Uncatalyzed	99.6	100.4	50.2	91.1
3	80	2.8	5.0781	99.2	100.8	50.4	91.2
4	90	3.9	5.0077	100.8	99.2	49.6	90.0
5	100	4.5	1.0053	103.8	96.2	48.1	87.3
6	100	4.3	3.1005	101.4	98.6	49.3	89.5
7	100	4.4	5.0074	100.2	99.8	49.9	90.5
8	100	4.5	10.0037	95.6	104.4	52.2	94.7
9	120	5.0	5.0036	106.0	94.0	47.0	85.3
10[a]	120	5.3	5.0032	102.4	97.6	48.8	88.5

[a] Powder of catalyst.

alytic particles with small metallic springs in a certain ratio (1:1.8 by weight); in this way a dimensional stability of the bed is achieved and no pressure drop was observed due to the high swelling ratio of the resin that correspond to a strong increase in volume [16]. The amount of catalyst loaded in the reactor is 10 g and the three run (11, 12 and 13) reported in Table 5 have been conducted without discharging it. Between two consecutive runs a catalyst washing with circulating hot oil for 30 min has been made. The outlet of the reactor is connected to the top of the tank in order to realize a circulation loop. The body of the reactor is heated with two 400 W resistances with a length of 150 mm each, also controlled by PID devices. The temperature of the system is monitored by two thermocouples respectively located on the top of the tank (liquid phase temperature) and at the outlet of the tubular reactor. The pressure of the vapor phase in the tank is monitored by a pressure transducer located also on the top of this device.

3. Results and discussion

3.1. Batch reactor

3.1.1. Diffusive phenomena

A preliminary investigation has been conducted in order to evaluate the influence of mass transfer limitations on the measured kinetic. All the experimental runs have been performed in conditions in which all diffusive phenomena can be neglected and the reactive system can be considered as in kinetic regime. The extent of the external diffusion has been verified by doing experiments at different stirring rates (500, 1000, 1200 and 1500 rpm at 120 °C), and a constant reaction rate has been observed above the threshold value of about 1200 rpm. The temperature for these specific runs has been fixed at 120 °C, the maximum of the temperature range explored, and with 5 g of catalyst. On the other hand, the influence of intraparticle diffusion has been verified by two comparative runs with catalyst as furnished by the vendor and the same catalyst finely powdered. No significant differences between conversion-time profiles of the two mentioned runs have been observed that corresponds to a negligible internal mass transfer limitation.

3.1.2. Development of the kinetic model

3.1.2.1. Uncatalyzed esterification. First of all, a preliminary study has been performed on the reaction in the absence of an heterogeneous catalyst (uncatalyzed reaction) with the scope of evaluating the contribution of the uncatalyzed reaction on the overall kinetics. Batch runs in the temperature range of 100–120 °C have been made with a molar ratio methanol/oleic acid of 8:1. The runs performed are described in Table 2. The collected experimental data, related to uncatalyzed reaction, have been correlated with a pseudo-homogeneous model by considering the reacting mixture as a single liquid phase and neglecting both the liquid–liquid eventual separation and the amount of volatiles (mainly methanol and water) that are present in the head space of the reactor. The kinetic expression for the reaction rate is the following:

$$r_{uc} = kC_A^2 C_M - k_{-1} C_A C_W C_E \simeq kC_A^2 C_M \tag{2}$$

where C_A and C_M are the liquid phase bulk concentrations of, respectively, oleic acid and methanol, k is the forward kinetic constant, k_{-1} is the reverse kinetic constant and r_{uc} is the reaction rate for the uncatalyzed reaction. The second order with respect to the reactant oleic acid is suggested by different authors [6,12,17] because this compound would act both as catalyst (in homogeneous phase) and reactant. In derivation of the expression (2) we have also neglected the reverse term of the equilibrium reaction because it have low influence in the simulations.

According to a modified Arrhenius equation, the reaction rate can be expressed as a function of temperature in the following way:

$$k = k^{ref} \exp\left[\frac{E_A}{R}\left(\frac{1}{T^{ref}} - \frac{1}{T}\right)\right] \tag{3}$$

In expression (3) k^{ref} is the kinetic constant at a reference temperature T^{ref} chosen at 373.16 K while R is the universal gas constant.

The mass balance for the isothermal batch reactor is then defined through the following system of ordinary differential equation (ODE), one for each component in the reacting system, to be solved starting from initial values of the concentrations:

$$\frac{dn_i}{dt} = \nu_i r_{uc} V_L \quad \text{with } i = A\,(\text{oleic acid}),\ \text{M}\ (\text{methanol}),\ \text{E}\ (\text{methyl ester}),\ \text{W}\ (\text{water}) \tag{4}$$

where n_i is the number of moles of the component i, ν_i is the corresponding stoichiometric coefficient i, V_L is the reaction volume evaluated with the ideal hypothesis of volumes additivity and using the densities of each component at the reaction temperature.

The kinetic parameters in expressions (2)–(4) have been evaluated by nonlinear fitting minimizing the following objective function represented by a quadratic mean square error between the experimental and calculated acidities.

$$RMS = \sqrt{\frac{1}{N}\sum_{i=1}^{N}(a_i^{exp} - a_i^{calc})^2} \tag{5}$$

Fourth order Runge-Kutta method was used to integrate the ODE system (4) at each iteration of the minimization algorithm used in nonlinear least squares fitting.

In Table 3 the values of kinetic parameters for the uncatalyzed esterification reaction are reported. An activation energy of about 16 kcal/mol has been found, in agreement with the values, for similar reactive systems, respectively obtained by Popken [12] for acetic acid esterification and by Sanz [17] for lactic acid esterification.

Table 3
Kinetic parameters of the uncatalyzed esterification.

k^{ref} (ref = 100 °C)	88.98 cm^6 mol^{-2} min^{-1}
Activation energy E_A	16.48 kcal/mol
Pre-exponential factor A	4.05×10^{11} cm^6 mol^{-2} min^{-1}
RMS error	0.854

3.1.2.2. Catalyzed esterification. Different catalytic runs have been performed by using Amberlyst 15 as catalyst by changing reaction temperature and catalyst concentration, as it can be seen in Table 2.

For the description of the experimental data two kinetic models have been tested. The first model (model 1, PH) is represented by a simple pseudo-homogeneous reversible expression for the reaction rate according to which the eventual presence of two liquid phases is neglected and also the solid phase (the catalyst) is lumped into the single hypothetical phase. As in the case of the uncatalyzed reaction, also the effects related to the vapor–liquid equilibrium are neglected. On the basis of these assumptions the model resulted very simple and suitable to be easily adapted to other reactor configurations. For this reason this model is popular and is frequently adopted in the literature [6,9,12,13,17].

The kinetic expression on which the model is based is the following:

$$r_{cat} = k_{cat} C_A C_M - k_{-cat} C_E C_W \quad (6)$$

where r_{cat} is the reaction rate for the catalyzed reaction, k_{cat} and k_{-cat} represent, respectively, the kinetic constants of the forward and the reverse reaction that can further been expressed in an Arrhenius form similar to Eq. (3).

In this case the mass balance for the batch reactor must be slightly modified, for taking into account the two contributions to the overall conversion of acid into the corresponding methylester: the uncatalyzed plus the catalyzed term. Therefore, the ODE system is now the following:

$$\frac{dn_i}{dt} = \nu_i (r_{uc}\, V_L + r_{cat} W_{cat}) \quad (7)$$

where W_{cat} is the mass of catalyst used. By minimizing the mean square error on the acidities collected in all the experimental runs of this type, the set of kinetic parameters can be evaluated and the corresponding values are reported in Table 4.

The described pseudo-homogeneous model, generally, interpret the experimental data of oleic acid conversion versus time with a sufficient accuracy but the agreement between the data and the model is unsatisfactory for the runs performed with different catalyst concentrations when the reactive system approaches the equilibrium. The equilibrium concentration, in this case, is described with an absolute error of about 5% on the final acidity value that corresponds to a relative uncertainty of 100%. Moreover, the activation energy for the reverse reaction (see Table 4) has no physical meaning being too low. This can probably be attributed to the fact that the kinetic constants in this model are only apparent being mathematical combination of a model based on a more realistic reaction mechanism.

A second approach for the description of the experimental data has been based on the development of a more complex model (model 2, ER) in which the adsorption on the catalyst of the reagents and products and a mechanism of the Eley-Rideal type have been accounted for. According to this model the reaction occurs between the oleic acid adsorbed on the catalyst surface and methanol coming from the bulk. A similar mechanism has already been proposed in the literature for Amberlyst 15 catalyst but for different reactions involving, for example, acetic acid [12,13]. The hypotheses on which the model is based can be summarized in the following point: (i) the resin is considered as an heterogeneous catalyst on which surface the adsorption of methanol, water, oleic acid and methyloleate occurs according to a Langmuir isotherm. The triglycerides present are considered as non-adsorbing compound. (ii) The adsorption equilibrium constants are assumed as temperature independent in the investigated temperature range; (iii) the rate-determining step in the overall reaction rate is the reactive event between adsorbed oleic acid and methanol coming from the bulk phase (Eley-Rideal step).

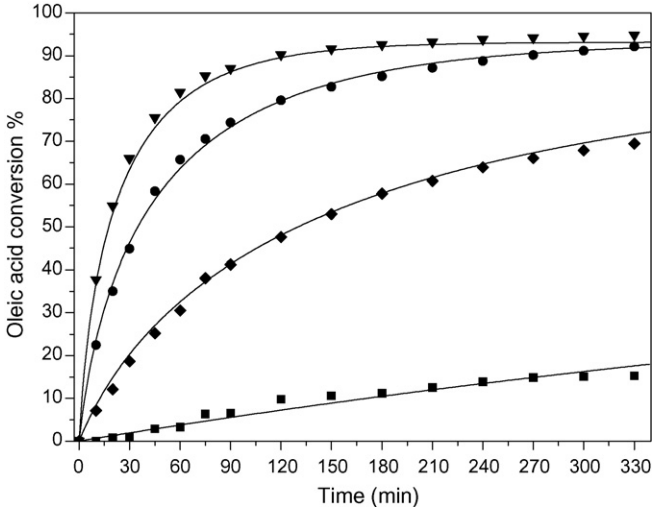

Fig. 3. Experimental batch run. Acid oil = 200 g at 50% of acidity. Methanol: oleic acid molar ratio = 8:1. (■) Uncatalyzed reaction at 100 °C. (♦) 5 g of catalyst at 80 °C. (●) 5 g of catalyst at 100 °C. (▲) 10 g of catalyst at 100 °C. Solid lines represent model simulation.

On the basis of the mentioned assumptions, the following kinetic rate law can be derived:

$$r_{cat} = \frac{k_{cat}\, b_A C_A\, C_M - k_{-cat}\, b_E C_E C_W}{1 + b_A C_A + b_M C_M + b_E C_E + b_W C_W} \quad (8)$$

where b_i are the adsorption equilibrium constants related to each component. The mass balance for the reactor is the same as expressed by relation (7).

The parameters estimation procedure is basically the same used for the previous model and the corresponding values of the obtained parameters are again reported in Table 4. In Fig. 3 the conversion-time profiles for runs performed at different temperatures are reported. As it can be seen, the agreement between the experimental and calculated data is very satisfactory and the obtained kinetic parameters are physically meaningful. The kinetic parameters reported in Table 4 are applicable, for both PH and ER models, in the following ranges of experimental conditions:

Table 4
Results of the kinetic study for catalyzed esterification.

Model	NP	Kinetic parameters				Absorption parameters				Statistics		
		k_{cat}^{rif}	E_A^{cat}	k_{-cat}^{rif}	E_A^{-cat}	b_M	b_A	b_W	b_B	RMS	R^2	F_{test}
1 (PH)	4	185.0	15.78	212.6	6.3×10^{-6}	–	–	–	–	10.71	0.809	113
2 (ER)	8	131.6	17.83	161.8	8.76	49.16	3.38	3537	1.59	7.28	0.912	266

NP = number of parameters. [k_{cat}^{ref}], [k_{-cat}^{ref}] (for PH model) = cm^6 mol^{-1} g$_{cat}^{-1}$ min^{-1}; (for ER model) = cm^3 g$_{cat}^{-1}$ min^{-1}, [E_A^{cat}], [E_A^{-cat}] = kcal mol^{-1}. [b_i] = cm^3 mol^{-1}.

Table 5
Operative conditions of experimental runs in packed bed loop reactor.

Run	Step number and duration	OA (g)	SO (g)	MeOH (g)	Molar ratio MeOH/OA	Recycle flow rate (dm^3/h)	T_1 (°C)	T_2 (°C)	T_3 (°C)	P (bar)
11	1°–1 h	147.6	152.4	138.4	8.3:1	1.5	125	125	110	6
12	1°–1 h	151.5	148.5	51	3:1	1.5	130	120	108	4.5
	2°–1 h	0	0	21.1	3:1	1.5	130	125	103	3.5
	3°–1 h	0	0	6.9	3:1	1.5	130	126	101	2.2
13	1°–1 h	150.9	149.1	34	2:1	3	130	121	105	3.7
	2°–1 h	0	0	21.1	3:1	3	130	121	103	3.3
	3°–1 h	0	0	8.6	3:1	6	130	126	100	3.2

T_1 = temperature of liquid in the tank. T_2 = temperature of gas in the tank. T_3 = temperature of packed bed reactor. OA = oleic acid. SO = soybean oil.

temperature 80–120 °C; catalyst amount 1–10 g/100 g of oleic acid; pressure 1–7 bar; initial acidity 50% by weight of oleic acid. For what concerns the adsorption constants, the highest value has been estimated, as expected, for water while methanol and even more oleic acid and ester have lower values. This behavior can be attributed to the high affinity of the resin toward water rather than the other components present.

A statistical analysis has been performed with the aim of discriminate between the two considered models and the related results are reported in Table 4. From this table it is possible to observe that the Eley-Rideal mechanism based model (model 2, ER) describes the experimental data with a higher value of the correlation coefficient R^2 and a root mean square error that is lower even if this model involves the use of more adjustable parameters. At last, in Table 4 is also reported the computed values for the F-test [18] according to which the E-R model (model 2) resulted superior to the simpler P-H model (model 1) in the description of experimental data (lower RMS and higher R^2 values) not only for the increased number of adjustable parameters, but also from a statistical point of view, showing a higher value of this statistical parameter [18].

3.2. Packed bed loop reactor

The second part of the present work has been devoted to a different reactor configuration, packed bed loop reactor (PBLR), which scheme is reported in Fig. 2. The experimental condition for the runs performed in this particular device are reported in Table 5 while other reactor and packing characteristics are summarized in Table 6. Moreover, some multistep runs have been performed with the aim to shift to the right the reaction equilibrium, removing water from the reactor. The details of these runs are reported in Table 5 (runs 12 and 13). In these runs, three subsequent reaction steps have been made. Between each step, water formed during the reaction and residual unreacted methanol were removed by stripping with a nitrogen flow stream. Then, fresh methanol was added and a successive reaction step was started. The duration of stripping phase was about 15 min. After the stripping, when the following step was started, fresh methanol was added to the system in a certain molar ratio with respect to the residual acidity from the previous reaction step. In particular, in these multistep runs, a reduced amount of methanol was used, with respect to the batch runs, and with the aim to lowering the separation costs of an eventual industrial operation in which the unreacted methanol should be purified from water and recycled.

Table 6
Characteristics of packed bed loop reactor.

Catalyst loading	10 g
Spring loading	18 g
Catalytic bed height	31.6 cm
Reactor internal diameter	1 cm
Weight ratio spring/catalyst	1.8
Catalytic bed volume	24.8 cm^3
Void factor	0.21
Tank volume	1 dm^3

3.2.1. Development of PBLR model

A mathematical model has been developed for the quantitative description of the performances of the loop reactor. A preliminary application of the Mears criterion [19] in a typical condition of this second set of experimental runs has shown the intervention, in a certain amount, of an external mass transfer limitation (Mears ratio between 0.7 and 0.9). The hypotheses on which this model is based can be summarized as follows: (i) the esterification reaction occurs both in the liquid reservoir tank and in the tubular reactor. In the tank the only contribution to the oleic acid conversion is the uncatalyzed reaction that was assumed in kinetic regime being the stirring rate the same adopted for the runs performed in batch reactor. (ii) In the tubular packed bed reactor, the chemical reaction was affected by external mass transfer limitation occurring from the bulk liquid phase to the catalyst surface; (iii) the tubular reactor was in unsteady-state conditions and was modeled through a CSTR-in-series approach. A total of 10 CSTR cells in series was found sufficiently accurate and in each cell the contribution of both uncatalyzed and catalyzed reaction (Eley-Rideal kinetics model 2, ER) was accounted for; (iv) the vapor–liquid and the eventual liquid–liquid phase equilibria have been neglected. On the basis of the mentioned hypotheses, a model was developed according to the scheme reported in Fig. 4 and described in details in the following.

3.2.2. Mass balance in the recycle tank

In the reservoir tank a mass balance related to each involved chemical specie has been written, with the exclusion of triglyc-

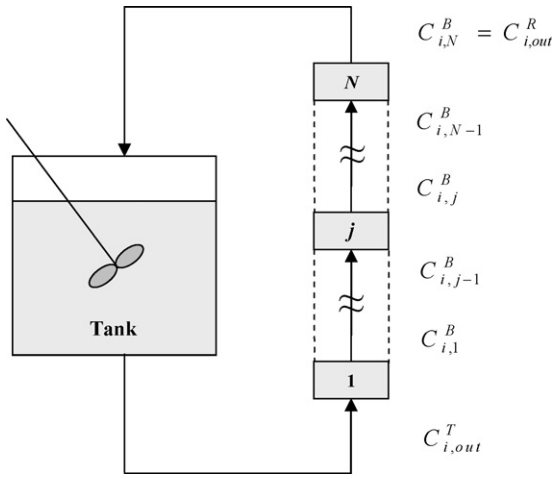

Fig. 4. Cell scheme for PBLR. Subscripts: j = cell number; N = final cell; i = component; superscripts: T = tank reactor; B = packed bed reactor.

erides that can be considered as inert material, by considering the contribution of the uncatalyzed reaction in chemical regime. The related differential equations obtained are the followings:

$$\frac{dn_i^T}{dt} = Q_R C_{i,out}^B - Q_R C_{i,out}^T - \nu_i r_{uc}^T V_L^T \quad (9)$$

where Q_R is the recirculation flow rate, $C_{i,out}^R$, $C_{i,out}^T$ are respectively the components concentrations at the outlet of the reactor and of the tank, r_{uc}^T is the uncatalyzed reaction rate and V_L^T is the liquid phase volume in the tank. The initial conditions for the integration of ODE system (9) by considering that at zero time both the tank and the void space in the tubular reactor are filled with the reactant mixture of equal composition. In this case we can write:

$$n_i^T(t=0) = \frac{m_i}{M_i}\left(\frac{V_L^{TOT} - V_L^B}{V_L^{TOT}}\right) \quad \text{(initial conditions)} \quad (10)$$

In expression (10) m_i is the mass of ith component initially charged in the tank, V_L^{TOT} is the total liquid volume at the temperature of the tank, V_L^B is the void volume in the packed bed reactor available for the liquid flow. This volume was calculated by introducing the void fraction ε of the bed as follows:

$$V_L^B = V^R \varepsilon \quad (11)$$

where V^R is the geometric volume of the empty tubular reactor, without catalyst or springs. Finally, it is possible to define the concentration of the different components in the tank:

$$C_{i,out}^T = \frac{n_i^T}{V_L^T} \quad (12)$$

3.2.3. Mass balance in the packed bed reactor

As said before, the tubular reactor is approximated as a certain number of CSTR in series, each of them operating in transient conditions. With this approach it is possible to transform a rigorous system of partial differential equation expressing mass balances into an approximate, but easier to solve, ODE system. Moreover, the reaction in the single cell is considered as the sum of two contributions, catalyzed and uncatalyzed, and is potentially affected by liquid–solid mass transfer resistance by diffusion. The mass balance equation assumes, therefore, then the following form:

$$V_L^C \frac{dC_{i,j}^B}{dt} = Q_R C_{i,j-1}^B - Q_R C_{i,j}^B + \nu_i (r_{uc,j}^B V_L^C + r_{cat,j} W_{cat}^C) \quad (13)$$

In Eq. (13), V_L^C and W_{cat}^C are, respectively, the liquid volume and the catalyst mass contained in each cell. Assuming that a pseudo-steady state holds for the mass transport, the amount of each reagent consumed by the reaction must be equal to the amount transferred by diffusion from bulk to the solid surface. This concept is expressed mathematically by relation (14).

$$k_S a_S (C_{i,j}^B - C_{i,j}^S) = -\nu_i r_{cat,j} C_{cat} \quad (14)$$

where k_S is the mass transfer coefficient, a_S is the specific interface area ($cm^2\ cm^{-3}$), estimated as the external geometric surface area of the resin per unit of reactor volume and assuming that the swollen resin particle are rigid spheres. Other notation for components concentration is the following: $C_{i,j}^S$ is the concentration of ith component on the resin surface in the jth cell and C_{cat} is the catalyst concentration defined as mass of catalyst per unit of reactor volume. The two contributions to the reaction rate in the single cell can be written as follows:

$$r_{nc,j}^B = k (C_{A,j}^B)^2 C_{M,j}^B \quad (15)$$

$$r_{cat,j} = \frac{k_{cat}\ b_A C_{A,j}^S\ C_{M,j}^S - k_{-cat} b_E C_{E,j}^S C_{W,j}^S}{1 + b_A C_{A,j}^S + b_M C_{M,j}^S + b_E C_{E,j}^S + b_W C_{W,j}^S} \quad (16)$$

At last, for the complete definition of the PBLR model, we need also an estimation of the liquid–solid mass transfer coefficient k_S, the only unknown parameter being the kinetics the one determined by interpreting the batch runs previously described. The estimation of k_S can be done both from literature correlation and from regression analysis of the experimental data (PBLR runs) considering the mass transfer coefficient as an adjustable parameter. In the present work, the correlation proposed by Nitta et al. [20], represented by the following expression:

$$Sh = 0.7 Re_p^{0.39} Sc^{0.50} \quad [1 < Re_p < 100] \quad (17)$$

has been used.

The particle Reynold number is calculated by the following expression:

$$Re_p = \frac{d_p U^B \rho_{mix}}{\eta_{mix}} \quad (18)$$

where d_p is diameter of resin particle (0.08 cm), U^B is linear velocity of mixture through the bed, ρ_{mix} and η_{mix} are density and viscosity of mixture.

The range of particles Reynolds number in which this correlation was developed is compatible with our experimental runs ($13 < Re_p < 56$) and the correlation should furnish a suitable estimation of k_S ($0.030 < k_S < 0.053\ cm\ min^{-1}$).

In our calculations this parameter was referred to the diffusion of oleic acid and was assumed, as a first approximation, the same for all the components. In the application of Eq. (17) to the estimation of mass transfer coefficient, pure components properties depending on temperature and composition like viscosity and density have been evaluated by using the databank of a commercial process simulator (Chemcad 5.2). The properties of the mixture have been evaluated according to Reid et al. [21] for what concerns viscosity and density while the diffusivity has been calculated as reported by Santacesaria et al. [10].

In Fig. 5, the simulation results of run 11 in comparison with the experimental data of acidity by considering, for the packed bed, both a kinetic and a diffusion-controlled regime (averaged particle Reynolds number of 48, middle of the range for Nitta correlation) are reported, as an example. From this figure we can observe that the behavior of the two regimes (kinetic, diffusion limited) are quite similar and consequently the PBLR technology allows to operate in conditions that are near to the kinetic regime, in opposite to what occurs in a continuous tubular reactors operating at high conversion

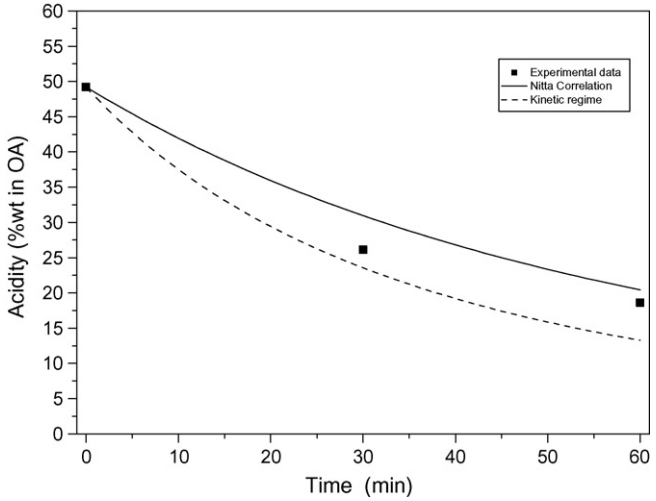

Fig. 5. Simulation of acidity profiles for run 11. (■) Experimental data. (- - -) Simulation with kinetic regime. (—) Simulation with Nitta correlation.

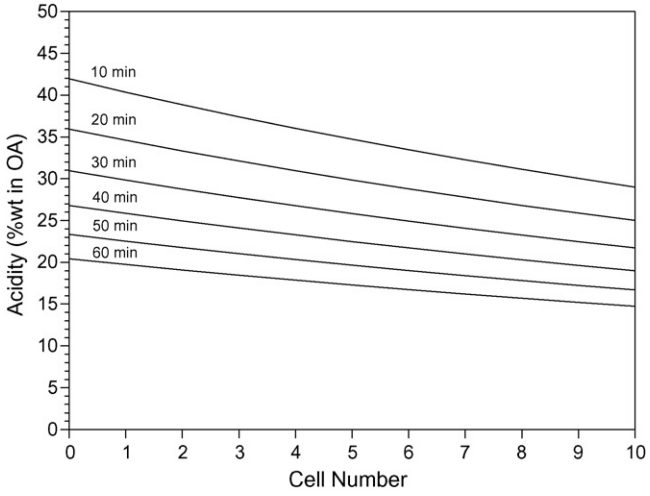

Fig. 6. Simulation of acidity profiles in packed bed reactor at different times of reaction for run 11.

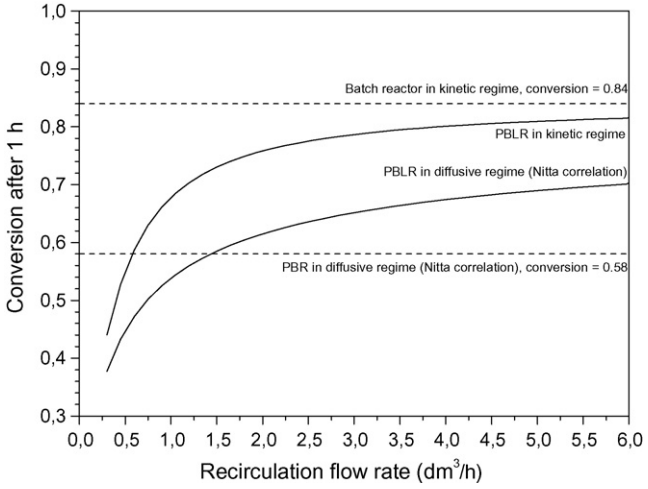

Fig. 8. Comparison of different reactor configurations. Simulation conditions: reaction time 1 h, acid oil processed 300 g, initial acidity 50%, molar ratio methanol/acid 8.3:1, temperature 110 °C, mass of catalyst 10 g.

in which mass transfer limitation strongly affect the performances of the system [10].

In Fig. 6 are reported some simulation results in terms of axial acidity profiles at different instant of time during the reaction evolution. It is possible to appreciate that the axial acidity profile (represented in terms of cell numbers in Fig. 6) evolves during the time and while it is initially rather steep, it becomes more and more flatten as the esterification reaction proceeds. This better explains the ability of the developed PBLR model to represent the dynamics of the system and, in a future perspective, this aspect should be validated by sampling the reactive mixture at different axial positions of the reactor.

In Fig. 7, typical results of a multistep run (with intermediate nitrogen stripping) are reported. In this case the final acidity is remarkably reduced with the further advantage that the overall amount of methanol used is strongly reduced with respect to the runs in batch conditions. This represents an improvement for what concerns the industrial operation being reduced the methanol/water separation cost. In the same figure, it is also possible to appreciate that the system is nearly in chemical regime due to the relatively high recirculation flow rates. In particular, in the second and in the third step of the reaction, the difference between the kinetic and the external diffusive regime (as predicted by Nitta correlation), become more and more less significant and the two regimes are substantially the same because in both cases reaction rates are very low. This aspect also shows that Nitta correlation is very suitable to describe the mass transfer effect in the described tubular reactor.

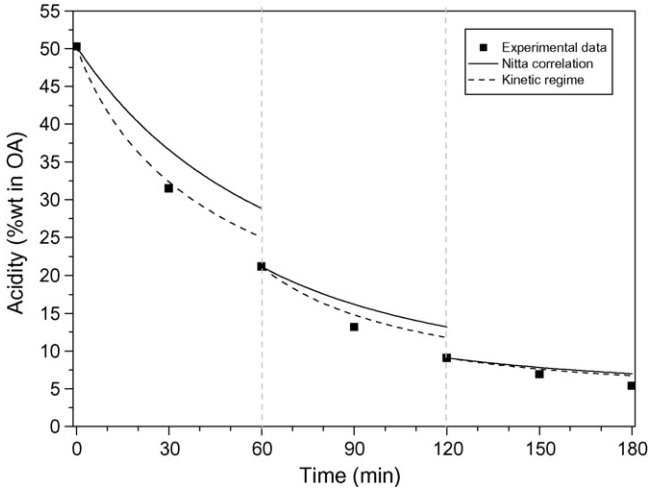

Fig. 7. Simulation of acidity profiles for run 13. (■) Experimental data. (- - -) Simulation with kinetic regime. (—) Simulation with Nitta correlation.

As a final consideration, a comparison between the different reactors configuration has been reported as simulations in Fig. 8. It was assumed that the three reactors (batch reactor, PBLR and packed bed reactor PBR) are operated in the same conditions for what concerns the amount of acid oil treated, the reactants ratio, the reaction time, the temperature and the catalyst weight. In this figure the conversion in the PBLR, after 1 h of reaction, is reported as a function of the overall recirculation flow rates for both kinetic and diffusive regime. For a comparison, is also reported the values of conversion calculated for both a batch reactor in pure kinetic regime and a PBR reactor in diffusive regime. In this last case, the feed flow rate of acid oil (0.3 kg/h) has been calculated in a way that, in 1 h, the same quantity charged in the batch and in the PBLR is processed. It is interesting to observe, as expected, that the behavior of conversion in the PBLR (kinetic regime) approaches that of batch reactor at high flow rates and, moreover, that the performances of this type of reactor (even if the diffusive limitations are taken into account) are better than PBR in correspondence of circulation flow rates higher than about 0.5–1.5 l/h. From another point of view, the PBLR reactor could usefully be adopted to overcome some limits or drawbacks that are typical of the stirred batch reactor. In this system very high catalyst concentrations are not feasible and a limit in stirring rate is required in order to avoid catalytic particle crushing.

4. Conclusions

In the present work different experimental runs have been described regarding the esterification of free fatty acids that are frequently present in low cost raw materials like waste oils or animal fats. Methanol was chosen as esterification agent and Amberlyst 15 as heterogeneous catalyst. The reaction has been performed by adopting two different reactors configuration that are a batch stirred tank reactor for determining the kinetics and a tubular packed bed loop reactor to evaluate the best operative conditions, also in comparison with previously studied continuous PBR. Data collected in the batch reactor were interpreted with a Eley-Rideal kinetic law taking into account also the contribution of the uncatalyzed reaction. The developed kinetic model (model 2, ER) resulted more satisfactory in simulating the experimental data than

the most popular pseudo-homogeneous model (model 1, PH) frequently used in the literature and the runs performed in the PBLR have been interpreted by using this kinetic model coupled with the mass transfer approach in which the mass transfer coefficient can be calculated with the Nitta correlation. By adopting a sufficiently high recirculation flow rate, as expected, the PBLR operates near to the chemical regime but without the negative effect of breaking the catalyst particles as it occurs in well stirred reactors and with performances higher than the continuous tubular reactor, operating at high conversions, that always works in diffusional regime. At last, it has been shown that with PBLR configuration with multi-steps operation, high FFAs conversion can be obtained also with low methanol/acid ratio so reducing the methanol–water separation costs.

Acknowledgements

The authors are grateful to Italian Ministry of Foreign Affairs (MAE, code 269/P/0127728) for it financial support in the developing the present work (Con il contributo del Ministero degli Affari Esteri, Direzione Generale per la Promozione e la Cooperazione Culturale).

References

[1] F. Ma, M.A. Hanna, Biodiesel production: a review, Bioresour. Technol. 70 (1999) 1–15.
[2] H. Fukuda, A. Kondo, H. Noda, Biodiesel fuel production by transesterification of oils, J. Biosci. Bioeng. 92 (2001) 405–416.
[3] J.H. Van Gerpen. Biological and Agricultural Engineering. University of Idaho, Moscow, ID, USA (Website: www.deq.state.mt.us.—*Biodiesel Economics. Montana Economics 2007*).
[4] D. Kusdiana, S. Saka, Kinetics of transesterification in rapeseed oil to biodiesel fuel as treated in supercritical methanol, Fuel 80 (2001) 693–698.
[5] M. Berrios, J. Siles, M.A. Martìn, A. Martìn, A kinetic study of the esterification of free fatty acids (FFA) in sunflower oil, Fuel 86 (2007) 2383–2388.
[6] C. Lacaze-Dufaure, Z. Mouloungui, Catalysed or uncatalysed esterification reaction of oleic acid with 2-ethyl texano, Appl. Catal. A: Gen. 204 (2000) 223–227.
[7] S. Pasias, N. Barakos, C. Alexopoulos, N. Papayannakos, Heterogeneously catalyzed esterification of FFAs in vegetable oils, Chem. Eng. Technol. 29 (11) (2006) 1365–1371.
[8] J.M. Marchetti, V.U. Miguel, A.F. Errazu, Heterogeneous esterification of oil with high amount of free fatty acids, Fuel 86 (2007) 906–910.
[9] R. Tesser, M. Di Serio, M. Guida, M. Nastasi, E. Santacesaria, Kinetics of oleic acid esterification with methanol in the presence of triglycerides, Ind. Eng. Chem. Res. 44 (2005) 7978–7982.
[10] E. Santacesaria, R. Tesser, M. Di Serio, M. Guida, D. Gaetano, A. Garcia Agreda, Kinetics and mass transfer of free fatty acids esterification with methanol in a tubular packed bed reactor: a key pretreatment in biodiesel production, Ind. Eng. Chem. Res. 46 (2007) 5113–5121.
[11] E. Santacesaria, R. Tesser, M. Di Serio, M. Guida, D. Gaetano, A. Garcia Agreda, F. Cammarota, Comparison of different reactor configurations for the reduction of free acidity in raw materials for biodiesel production, Ind. Eng. Chem. Res. 46 (2007) 8355–8362.
[12] T. Popken, L. Gotze, J. Gmehling, Reaction kinetics and chemical equilibrium of homogeneously and heterogeneously catalyzed acetic acid esterification with methanol and methyl acetate hydrolysis, Ind. Eng. Chem. Res. 39 (2000) 2601–2611.
[13] S.H. Ali, S.Q. Merchant, Kinetics of the Esterification of Acetic Acid with 2-Propanol: Impact of Different Acidic Cation Exchange Resins on Reaction Mechanism doi:10.1002/kin.20193, Published online (http://www.interscience.wiley.com).
[14] M. Mazzotti, B. Neri, D. Gelosa, A. Kruglov, M. Morbidelli, Kinetics of liquid-phase esterification catalyzed by acidic resins, Ind. Eng. Chem. Res. 36 (1997) 3–10.
[15] D. Gelosa, M. Ramaioli, G. Valente, M. Morbidelli, Chromatographic reactors: esterification of glycerol with acetic acid using acidic polymeric resins, Ind. Eng. Chem. Res. 42 (2003) 6536–6544.
[16] D. Siano, M. Nastasi, E. Santacesaria, M. Di Serio, R. Tesser, G. Guida, Method for forming a packing for resin catalytic packed beds, and so formed packing, WO 2006/046138 A1.
[17] M.T. Sanz, R. Murga, S. Beltràn, J.L. Cabezas, J. Coca, Autocatalyzed and ion-exchange-resin-catalyzed esterification kinetics of lactic acid with methanol, Ind. Eng. Chem. Res. 41 (2002) 512–517.
[18] J.R. Taylor, An Introduction to Error Analysis, 2nd revised ed., University Science Books, 1997.
[19] D.E. Mears, Tests for transport limitations in experimental catalytic reactors, Ind. Eng. Chem. Proc. Des. Dev. 10 (4) (1971) 541–547.
[20] D. Seguin, A. Montillet, D. Brunjail, J. Comiti, Liquid–solid mass transfer in packed beds of variously shaped particles at low Reynolds numbers: experiments and model, Chem. Eng. J. 63 (1996) 1–9.
[21] R.C. Reid, J.M. Prausnitz, B.E. Poling, The Properties of Gases & Liquids, 4th edition, McGraw-Hill, New York, 1987.